

Doping TiO₂ by Cr from tannery wastewater for improving its activity under visible light in the dye degradation

Endang Tri Wahyuni^{a*}, Sri Wahyuni^a, Mandrea Nora^a, Novianti Dwi Lestari^a, and Suherman Suherman^a

a)Chemistry Department, Faculty of Mathematics and Natural Sciences, Yogyakarta, Universitas Gadjah Mada Sekip Utara POB Bls 21, Yogyakarta, Indonesia, 55284

Received 30 November 2022; received in revised form 14 March 2023; accepted 19 May 2023 (DOI: 10.30495/IJC.2023.1973955.1980)

ABSTRACT

This paper deals with the comparison of the Cr (III) dopant from tannery wastewater to the Cr (III) from the pure salt solution on the character and activity of TiO₂. The doping was conducted by hydrothermal method, and the Cr-doped TiO₂ prepared was characterized by UV specular reflectance (SRUV), X-ray diffraction (XRD), and X-ray fluorescence instruments. The effect of the Cr (III) doping on the activity of the TiO₂ was evaluated by Congo red photodegradation. The research results reveal that Cr (III) doping on TiO₂ has been successfully reducing remarkably the band gap energy (E_g) from 3.13 eV to 2.64 eV, shifting into the visible region, and further noticeably improving TiO₂ activity. The effect of the Cr (III) doping from the wastewater is found to be slightly higher than that of the salt solution. The highest degradation of 10 mg/L Congo red in 50 mL solution, can be reached by applying 30 mg of the photocatalyst in 60 mins and at pH 7.

Keywords: Congo red dye, Cr, Doping, Photodegradation, Tannery wastewater, TiO₂

1. Introduction

TiO₂ is a photocatalyst possessing some excellent properties including strong oxidation power, high stability, low cost, and environmentally benign [1-15], allowing it to be frequently applied in the degradation of various organic pollutants [1-4] to form smaller and/or saver compounds. However, the weakness of TiO₂ associated with the poor adsorption, low surface area, rapid recombination of electron-hole pair [16], and the wideband gap energy (E_g) of 3.2 eV for the anatase type, allows it to work only in the presence of UV light and constrains its application under visible light, dominantly found in the sunlight [5-15]. Accordingly, improvement of the TiO₂ activity under visible light is essential, which has been intensively conducted by doping with, especially, transition metals, including Ni [5-6], Fe [7-8], Cu [9-10], Co [6], Mn [6], and Cr [11-16]. Through transition metal doping, a new band located in the gap between the conduction and the valence bands can be created in the TiO₂ semiconductor

structure, which narrows the gap [5-16]. As a result, the smaller band gap energy (E_g) is generated, which is equal to the power of the visible light, allowing TiO₂ to be more active under visible light compared to the undoped one [5,12,17].

Among the transition metal dopants, Cr (III) ions are reported to show a significant effect on the E_g reduction and visible responsive improvement of TiO₂ [11-16]. This is due to the smaller charge and ionic radii of Cr (III) than that of Ti(IV) ions [13] enabling Cr(III) to be doped effectively. In the Cr (III) doping, commercial chromium salts are always used, including Cr(NO)₃ [11, 13], Cr₂O₃ [14-16], and Cr (III) acetylacetonate [12], which are relatively expensive, causing the costly doping process. Accordingly, finding a cheap Cr(III) source is beneficial, and one of the cheap chromium sources is tannery wastewater containing high Cr(III) concentration [18-20].

In the tannery process, a large amount of Cr(III) salts as the tanning agent is used, but almost 40 % of the Cr(III)

*Corresponding author:

E-mail address: endang_triw@ugm.ac.id (E. T. Wahyuni);

is released into wastewater [18–20]. The chromium-containing wastewater disposed of in the environment without any proper treatment can create environmental problems and health disorders [19]. Drinking water polluted by Cr (III) ions for a long term, even if in trace levels, contributes to the development of several health diseases, such as malignancy, queasiness, loss of consciousness, renal failure, and elusive effects on metabolism and intelligence [19]. Removal of the Cr (III) from the tannery wastewater has been intensively conducted by adsorption with various adsorbents including cactus powder [18], coffee husk [19], and fruit waste [20]. In fact, at the end of the adsorption process, the adsorbent that has been saturated with the Cr (III), becomes a hazardous solid waste that generates new environmental problems. On the side, the high Cr (III) concentration is very potential to be used as Cr (III) dopant source. However, according to the best of our knowledge, the lack of reports of the use of tannery wastewater as a source of Cr dopant can be found.

Under the circumstance, in the present research, doping TiO₂ with Cr (III) from the tannery wastewater is studied. The activity of the Cr-doped TiO₂ under visible light is examined for Congo red dye degradation. The dye is selected as a pollutant model, because the dye is widely used in several industries including textile and other wearable materials [21–25], as well as in the laboratory for bacterial staining [22–24], leading it to be widely contained in the associated wastewater. It is frequently reported, that the presence of Congo red dye in the environment can create serious effects, such as biotic death, and human health problems including vomit, nausea, and diarrhea [20, 24].

Removal of Congo dye has been intensively reported by using a variety of methods such as adsorption [20], photo-Fenton [21], ozonation [22], and photocatalytic degradation over TiO₂ under UV light [23], as well as over Fe-doped TiO₂ in the presence of visible light [24]. However, degradation under visible light in the presence of TiO₂ doped with Cr element from tannery wastewater for removal of the Congo red dye is a lack of information.

In this study, the TiO₂ doping process by Cr (III) from leather tannery wastewater was carried out using the hydrothermal method, which is compared to the Cr (III) from the pure salt solution. In addition, the irradiation time, photocatalyst mass, and solution pH, in the degradation of Congo red dye are also optimized to find the best condition for the dye degradation.

2. Experimental

2.1. Materials

The main materials used in this research were TiO₂, Cr(NO₃)₃, and Congo red dye powder. The chemicals were purchased from Merck and used as received without further purification. The tannery wastewater was taken from a leather industry in Kotagede, Yogyakarta, Indonesia. The total concentration of total Cr in the tannery wastewater was determined by using a flame atomic absorption spectrophotometer at the associated wavelength. The concentration of total Cr in the tannery wastewater was found as approximately, 5200 mg/L.

2.2. Doping of TiO₂ with Cr (III) ions

The Cr doping was prepared by hydrothermal method. In the typical procedure, 0.8 grams of TiO₂ powder (= 10 mmole) was mixed with 50 mL of the tannery wastewater containing ≈ 5200 mg/L Cr (≈100 mmole/L) and was magnetically stirred for 15 mins to get a homogeneous mixture. Then the mixture was placed in a 250 mL autoclave, and heated at 150 °C under pressure slightly higher than 1 atm, for 6 h. The Cr-doped TiO₂ from the autoclave then was dried at around 100 °C to get dry powder [26]. The same procedure was repeated for doping Cr (III) from the commercial salt solution with the same concentration. The doped photocatalysts obtained were noted as TiO₂-Cr (WW) and TiO₂-Cr(CS) representing the Cr(III) from the tannery wastewater and the commercial salt, respectively.

2.3. Characterization

The crystal types and crystallinity of Cr-doped TiO₂ samples were detected by using a Shimadzu XRD-6000 X-ray diffractometer with a Cu-Kα target metal radiation source. The X-ray diffractogram patterns were collected at the angles of 2θ from 3°–80° with a scanning speed of 4°/minute. The UV-Vis specular reflectance spectra (SR) were recorded using a UV-visible spectrophotometer (JASCO, UV-670) in the wavelength range of 200–800 nm to determine the band gap energy (E_g) values.

2.4. Photodegradation of Congo red dye under visible irradiation

In this process, 30 mg of TiO₂, TiO₂-Cr (WW), and TiO₂-Cr (CS), photocatalysts were added into 50 mL of Congo red dye solutions having 10 mg/L. Then, a series of the mixture was put into a photodegradation device equipped with a tungsten lamp emitting visible light. The irradiation process was carried out for 60 minutes,

accompanied by stirring using a magnetic stirrer. After the desired time, the photocatalyst powder was separated from the solution using a centrifuge. The concentration of the degraded Congo red solution was measured with a UV-Visible spectrophotometer based on the respective standard curve. The effectiveness of the dye photodegradation was determined using the equation below:

$$E = \frac{C_0 - C_t}{C_0} \times 100\% \quad (1)$$

Where E is the effectiveness of decreasing the concentration of Congo red dye (%), C_0 is the initial concentration of Congo red dye (mg/L), and C_t is the final concentration of Congo red dye after photodegradation (mg/L). The same procedure was repeated for various weights of the doped-TiO₂, different reaction times, and pH variations in the dye solutions.

3. Results and Discussion

3.1. Characterization of the Cr-doped TiO₂

3.1.1. SRUV spectra

Table 1 The effect of Cr doping on the decreasing E_g of TiO₂

Photocatalyst	TiO ₂	TiO ₂ -Cr (CS)	TiO ₂ -Cr (WW)
λ (nm)	405	471	482
E_g (eV)	3.13	2.69	2.64

The SRUV spectra of Cr-doped TiO₂ and the un-doped TiO₂ are presented in **Fig. 1**. The wavelengths of the absorption edge of all samples were presented in **Table 1**, along with the band gap energy (E_g) values that were calculated by the Tauc plot method as seen in **Fig. 2** [14]. From the figure and the table, it is noticed that the absorption light of the TiO₂-Cr shifts from 404 nm to longer than 450 nm, entering the visible area, and consequently reducing the E_g value. The E_g decrease resulted from the narrowing gap due to the formation of a new band created by the dopant [5, 16].

The E_g decrease resulting from the Cr dopant from the tannery wastewater is found to be more effective than that of the commercial salt, for the same amount of the Cr doped. This difference may be caused by the fact that the tannery wastewater also contains protein residual from the tanned leather, which can provide carbon and nitrogen atoms to be doped into the TiO₂ crystal. It is frequently reported that the double dopants give more effective E_g decrease and enhancement in the activity than the single dopant [5].

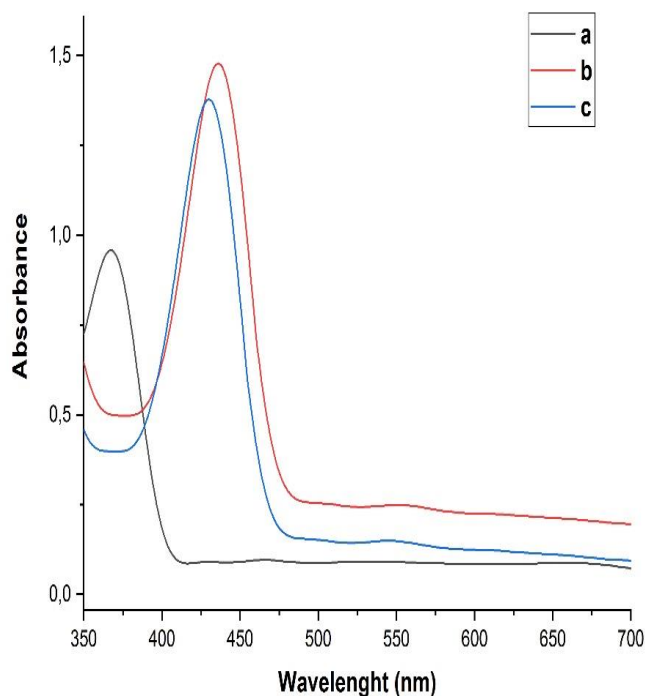


Fig. 1 The SRUV spectra of a) TiO₂, b) TiO₂-Cr (CS), and c) TiO₂-Cr (WW)

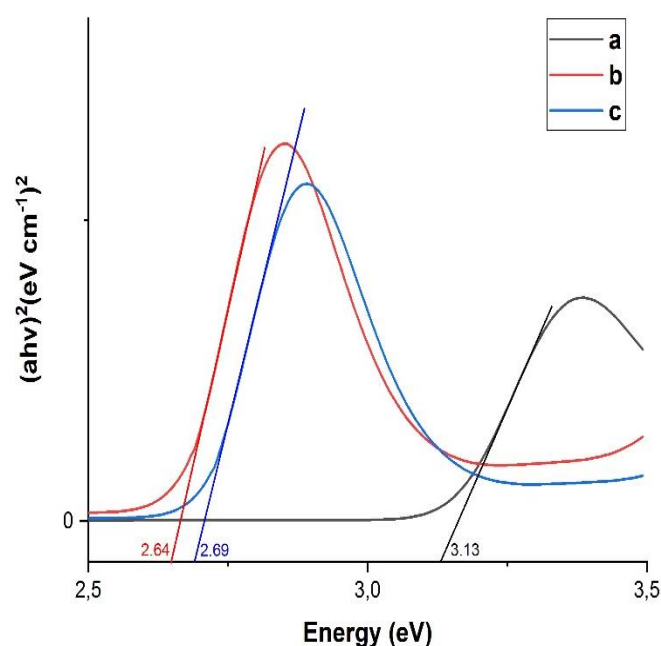


Fig. 2 The Tauc plot of a) TiO₂, b) TiO₂-Cr (CS), and c) TiO₂-Cr (WW)

3.1.2. XRD data

The diffraction patterns of TiO₂ and the Cr doped-TiO₂ both from tannery wastewater and commercial salt solution were displayed in **Fig. 3**. The diffraction patterns of the Cr-doped TiO₂ are similar to the pattern of the un-doped one without any new peaks. All of the samples can be well indexed to the anatase phase. The peaks at 25.31, 36.91, 37.81, 38.61, 48.01, 53.91, and 55.11 can be ascribed to (101), (103), (004), (112), (200), (105), and (211) planes of anatase, respectively (JCPDS Card No. 21-1272 [13, 14]). The absence of the new pattern indicates that the Cr dopant is diffused in the TiO₂ crystal lattice implying the success of the doping [14].

The doping is seen to reduce the intensities, inferring the lower crystallinity of TiO₂. It implies that doping leads to crystal distortion, inferring that the Cr doping has successfully occurred [13]. Similar findings have also been reported [5, 12, 16].

The Cr doping from the tannery wastewater shows a stronger effect on the TiO₂ crystallinity distortion, which may be caused by more dopants present in the tannery

wastewater. This XRD is in good agreement with their Eg data.

From the XRD data, the average crystallite size of TiO₂ can be determined by following the Debye-Scherrer formulae as shown below [11, 12, 16]:

$$D = \frac{k\lambda}{\beta \cos\theta}$$

Where D is crystallite size, K is shape factor (0.9), β is the Full-width half maxima (FWHM) (in radians), λ is the X-ray wavelength (1.5418 Å for Cu-K α radiation) and θ is the Bragg angle of diffraction. The results of the calculation are presented in **Table 2**.

Data in the table assigns that the Cr doping can enlarge the average crystallite size of the TiO₂. The increase in the size infers that the Cr doping follows the interstitial mechanism [16]. The larger size of the TiO₂-Cr from the wastewater can assign that the larger amount of the dopant, from Cr and the other atoms, have been doped into TiO₂.

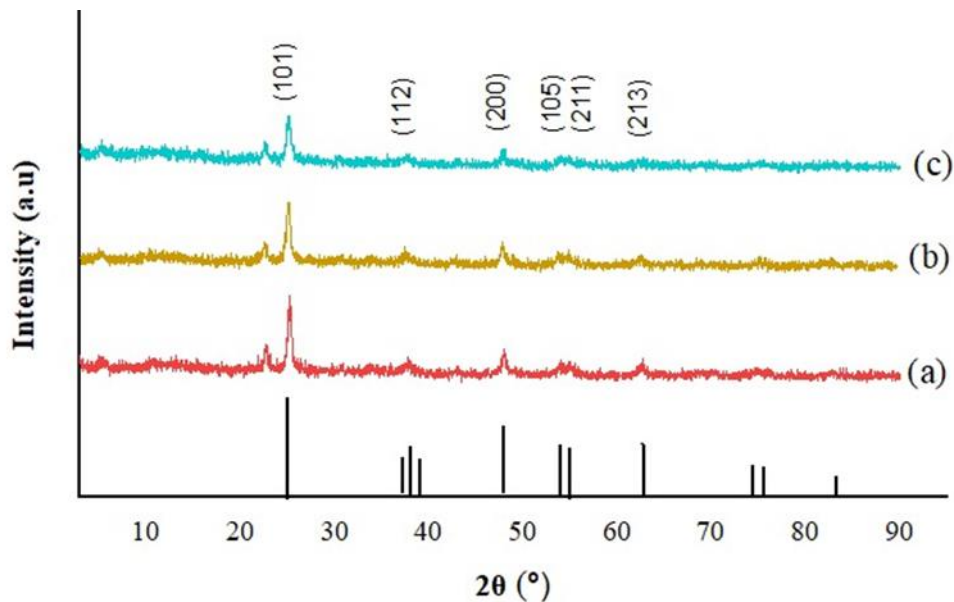


Fig. 3 XRD patterns of: a) TiO₂, b) TiO₂-Cr (1:CS), c) TiO₂-Cr (WW)

Table 2. Doping effect of the average crystallite size

Sample	2 θ	(β)	D (nm)
TiO ₂	25.18	0.18	47.26
TiO ₂ -Cr (CS)	25.14	0.16	53.16
TiO ₂ -Cr (WW)	25.02	0.14	60.74

3.1.3. XRF Data

Table 3 shows the chemical composition of the TiO₂ and TiO₂-Cr photocatalysts analyzed by XRF. There were some impurities detected on each photocatalyst, where TiO₂-Cr (WW) has the highest amount of impurities due to the tannery wastewater containing several elements, such as Na, C, N, and S. Chemical composition of TiO₂-Cr showing that Cr was successfully doped into the TiO₂ structure. The amount of Cr doped in the TiO₂-Cr (CS) and TiO₂-Cr (WW) is similar to the mole ratio of Ti: Cr preparation.

3.1.4. Influence of doping Cr on TiO₂

Fig. 4 illustrates the effectiveness of the dye photodegradation over different TiO₂ photocatalysts, both under visible (3a) and UV lights (3b). It can be seen in the figure that Cr doping, both from the wastewater and salt standard solution, can considerably improve the activity of TiO₂ whether under visible and UV lights in the dye degradation. The dye photodegradation under UV light is found to be higher than that under visible illumination.

The increase in TiO₂ activity under visible light after being doped with Cr resulted from the stronger visible absorption by the TiO₂-Cr than by TiO₂, due to its lower E_g of the doped TiO₂ emerging in the visible light. This stronger absorption of visible light stimulates TiO₂-Cr

to produce more holes or OH radicals, for more effective dye degradation. In contrast, the E_g value of TiO₂ is 3.20 eV, which enters UV light, limiting it in visible light absorption. Consequently, in the presence of a lower energy beam than its E_g, TiO₂ is not sufficiently capable of providing holes or OH radicals [13, 16].

Then, under UV exposure light, the TiO₂-Cr activity is also found to be higher than the undoped one. The Cr dopant may create a new band just below the conduction band [16] and has a partially empty d-orbital [13], enabling it to capture the electrons excited from the valence band. As a result, the recombination of the electrons and holes can be prevented, so that more holes and OH radicals are available for more effective dye degradation.

With the same photocatalyst, the higher dye degradation under UV light than under visible light is reasonable. Since the energy of the UV light is higher than that of the visible one, capable TiO₂ generates more holes and radicals. It is also notable that the activity of the TiO₂-Cr from the tannery wastewater is slightly higher than that of the standard solution. This data is the result of TiO₂-Cr that has lower E_g, and so that is able to stronger absorb the visible light. In addition, the TiO₂-Cr from the wastewater, which may also contain another dopant, can prevent charge recombination more effectively, providing more holes and OH radicals.

Table 3. Chemical composition of the photocatalyst determined by the XRF method

Photocatalyst	The elemental content (% w)		
	Ti	Cr	Others
TiO ₂	95.23	0	4.77
TiO ₂ -Cr (CS)	64.24	31.08	4.68
TiO ₂ -Cr (WW)	59.67	32.34	7.99

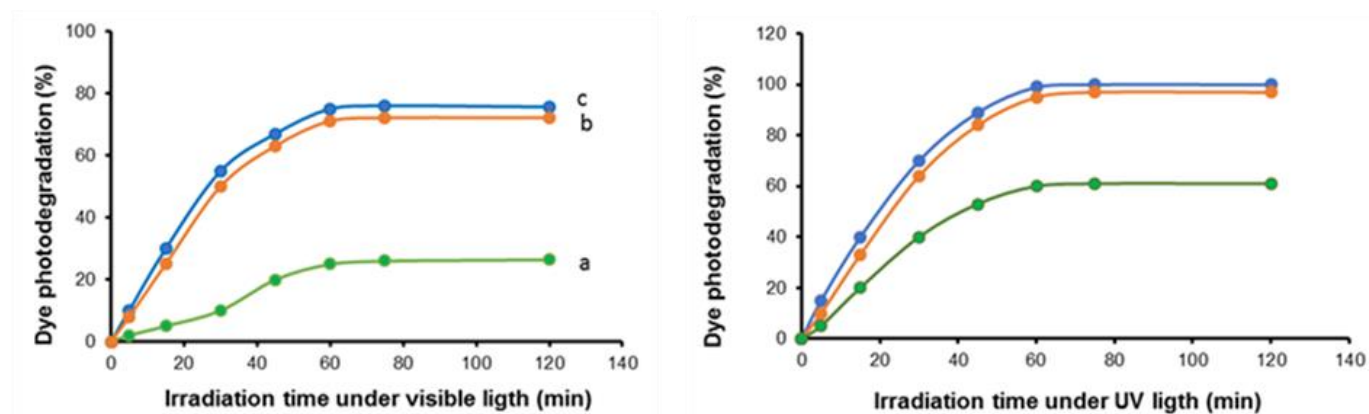


Fig. 4. The results of Congo red photodegradation over a) TiO₂, b) TiO₂-Cr (CS), and c) TiO₂-Cr (WW) (Dye concentration = 10 mg/L, dye solution volume = 50 mL photocatalyst weight = 30 mg, and pH = 7)

3.2. Photocatalytic activity of $\text{TiO}_2\text{-Cr}$ in photodegradation of Congo red under visible light

3.2.1. Influence of irradiation time

The effectiveness of Congo red dye photodegradation in the different irradiation times is also displayed in **Fig. 4**. An increase in dye photodegradation is observable with the extension of the irradiation time up to 60 mins. The longer the irradiation time, the more light is absorbed by the photocatalyst and water, so that a larger number of holes and OH radicals can be produced. When the irradiation time exceeds 60 minutes, where the photocatalyst has absorbed the visible light maximally, no addition of the OH radicals can be generated resulting same effectiveness of the dye photodegradation. Some Authors also reported a similar trend [5, 10, 12].

3.2.2. Influence of pH solution

The effectiveness of the Congo red dye photodegradation in the solution pH alteration can be seen in **Fig. 5**. The less effective dye degradation is observed at a very low pH. When the pH is advanced to increase up to 7, the dye degradation sharply enhances. The opposite trend of the degradation is notified as the further escalated the pH. The highest degradation is clearly observed at pH 7. At pH 2, the surface of the TiO_2 photocatalyst and the dyestuffs are positively charged, since the zero point charge pH of TiO_2 is 6.5 [10] and the isoelectric point of Congo red is found at pH 3 [17]. The same charges cause repulsion of the dye by TiO_2 , inhibiting the dye adsorption on the

photocatalyst surface. Consequently, low degradation is obtained.

In the solution with pH 3, the dye is in a neutral charge, while the TiO_2 surface is predominantly positive, allowing them to interact, which results in higher degradation. Further increasing pH, the positive charges of the TiO_2 may be reduced to form the uncharged surface, while the dye starts to have a negative charge. This condition is conducive for dye adsorption and so the effective degradation. When the solution is set at a pH higher than 7, most of the TiO_2 surface charges, as well as the dye charges, are in the negative form that prevents TiO_2 to adsorb the dye. Consequently, the lack of Congo red dye can be degraded.

3.2.3. Influence of photocatalyst mass

As shown in **Fig. 6**, the dye photodegradation effectiveness increases sharply with the addition of photocatalyst mass, but the less effective dye photodegradation is noticeable when the photocatalyst mass is further enlarged. It is important to note that the mass of the $\text{TiO}_2\text{-Cr}$ photocatalyst controls the number of OH radicals formed. The OH radicals are the reactive species that are responsible for dye degradation.

As the photocatalyst mass increases, more OH radicals are available, so the higher effectiveness of the photodegradation process proceeds. However, when the photocatalyst mass is in excess, the turbidity in the solution also raises, which can block the light entering the dye solution [10]. Therefore, the number of OH radicals formed become lesser, declining the effectiveness of the Congo red photodegradation.

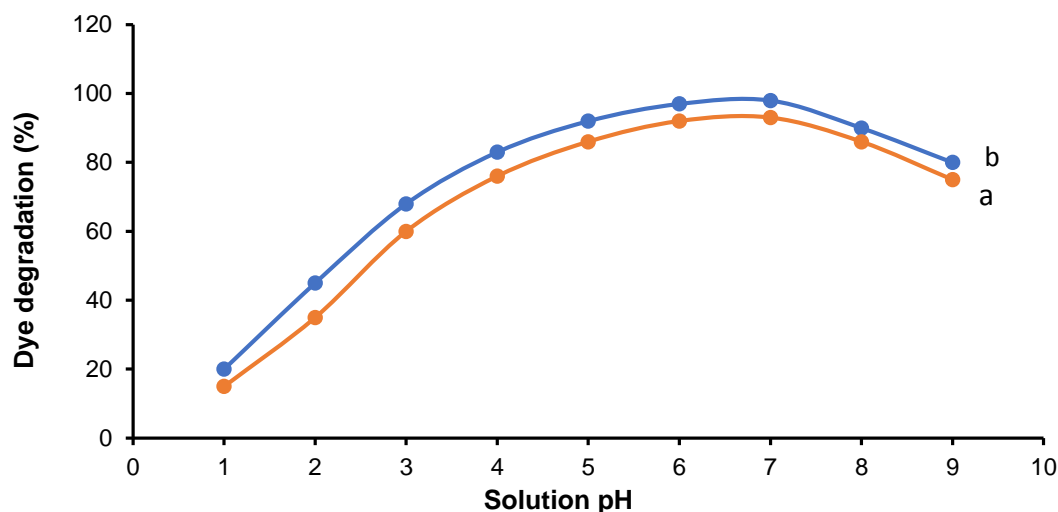


Fig. 5. The influence of the pH solution on the photodegradation of Congo red by: a) $\text{TiO}_2\text{-Cr}(\text{CS})$ and b) $\text{TiO}_2\text{-Cr}(\text{WW})$ (Dye concentration = 10 mg/L, dye solution volume = 50 mL photocatalyst weight = 30 mg, and irradiation time = 60 mins)

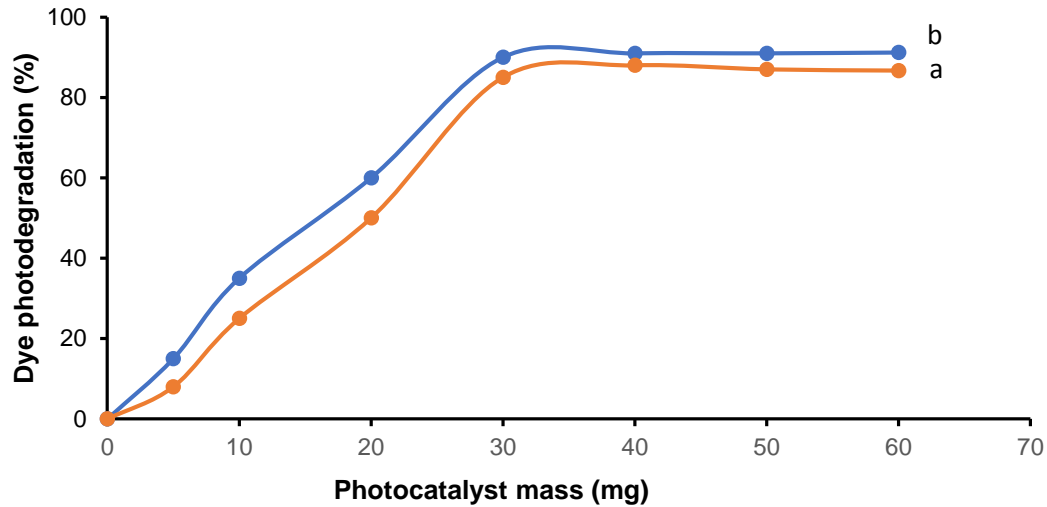


Fig. 6. Influence of the photocatalyst mass on the photodegradation of Congo red by: a) TiO₂-Cr(CS) and b) TiO₂-Cr(WW) (Dye concentration = 10 mg/L, dye solution volume = 50 mL irradiation time = 60 mins, and pH = 7)

3.2.4. Stability test of the TiO₂-Cr

The stability of the TiO₂-Cr has been checked by measuring the concentration of the Cr dissolved from the photocatalyst during the dye photocatalytic degradation process. The photocatalyst tested was TiO₂-Cr (WW) showing the best performance, and the results are presented in **Fig. 7**. It is seen in the figure that during the photocatalysis degradation, a very low amount of Cr dissolved is detected. The longer the irradiation time, the more Cr dissolved is slightly increased. It is believed hence that the Cr dopant has high stability.

4. Conclusions

It can be concluded that Cr (III) ions both from the leather tannery wastewater and from the Cu(NO₃)₃ salt solution have been successfully doped on TiO₂. The Cr

doping on TiO₂ has significantly reduced the E_g values from 3.13. eV to 2.64 eV, emerging into the visible region, and further can remarkably enhance the activity of TiO₂ under visible light for Congo red dye degradation. The effect of the Cr (III) dopant from the wastewater on the character and activity of TiO₂ is found to be slightly higher than that of Cr (III) from the standard solution. The best condition for the Congo red dye degradation over TiO₂-Cr, both from the tannery wastewater and the standard solution, can be reached by employing 30 mg of the photocatalyst, in 60 mins, and at pH 7, that is about 90-93% of the 10 mg/L Congo red dye in 50 mL of the solution. It is clearly proven that hazardous tannery wastewater containing high Cr (III) concentration, can be converted into a useful material, such as a dopant, for preventing environmental dye pollution.

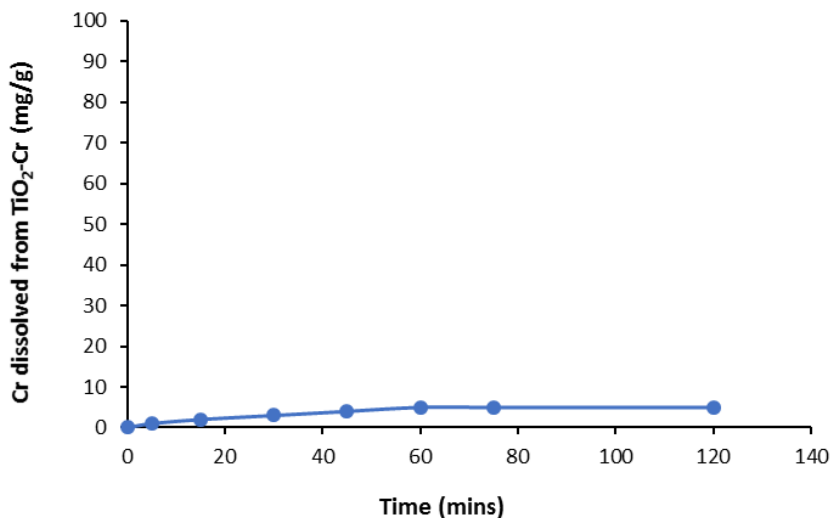


Fig. 7. The amount of the Cr dopant dissolved from the doped photocatalyst during the photocatalysis degradation process.

Acknowledgements

The authors thank the Ministry of Education and Culture of the Republic of Indonesia through the National Competition Grant of Basic Research Schema for supporting this project through contract number: 1846/UN.1/DITLIT/dit-Lit/PT.01.03/2022, May 27, 2022

References

- [1] A. Eslami, M.M. Amini, A.R. Yazdanbakhsh, A. Mohseni-Bandpei, A.A. Safari, A. Asadi, *J. Chem. Technol. Biotechnol.* 91 (2016) 2693–2704.
- [2] X. Zhu, D. Zhou, L. Cang, Y. Wang, *J. Soils Sediments* 12 (2012) 376–385.
- [3] M.L.P. Dalida, K.M.S. Amer, C.C. Su, M.C. Lu, *Environ. Sci. Pollut. Res.* 21 (2014) 1208–1216.
- [4] S. Wu, H. Hu, Y. Lin, J. Zhang, Y.H. Hu, *Chem. Eng. J.* 382 (2020) 122842.
- [5] M. Shaban, A.M. Ahmed, N. Shehata, M.A. Betiha, A.M. Rabie, *J. Colloid Interface Sci.* 555 (2019) 31–41.
- [6] R. Kaur, P. Singla, K. Singh, *Int. J. Environ. Sci. Technol.* 15 (2018) 2359–2368.
- [7] M.L. Matias, A. Pimentel, A.S. Reis-Machado, J. Rodrigues, J. Deuermeier, E. Fortunato, R. Martins, D. Nunes, *Nanomaterials* 12 (2022) 1–23.
- [8] S. Sood, A. Umar, S. Kumar, S. Kumar, *J. Colloid Interface Sci.* 450 (2015) 213–223.
- [9] H. Lee, H.S. Jang, N.Y. Kim, J.B. Joo, *J. Ind. Eng. Chem.* 99 (2021) 352–363.
- [10] K.P. Suwondo, N.H. Aprilita, E.T. Wahyuni, *React. Kinet. Mech. Catal.* 135 (2022) 479–497.
- [11] R.A. Saleh, O.N. Salman, M.O. Dawood, *J. Nanostructures* 11 (2021) 678–683.
- [12] X. Li, Z. Guo, T. He, *Phys. Chem.* 15 (2013) 20037–20045.
- [13] M. Asemi, S. Maleki, M. Ghanaatshoar, *J. Sol-Gel Sci. Technol.* 81 (2017) 645–651.
- [14] L. Yuan, X. Weng, M. Zhou, Q. Zhang, L. Deng, *Nanoscale Res. Lett.* 12 (2017) 597–604.
- [15] G.C. Vásquez, D. Maestre, A. Cremades, J. Ramírez-Castellanos, E. Magnano, S. Nappini, S.Z. Karazhanov, *Sci. Rep.* 8 (2018) 1–12.
- [16] A. Nezamzadeh, M. Khorsandi, *J. Hazard. Mater.* 176 (2010) 629–637.
- [17] I. Ben Jemaa, F. Chaabouni, A. Ranguis, *J. Alloys Compd.* 825 (2020) 153988.
- [18] W. H. Rimawi, S. Shaheen, H. Salim, *Orient. J. Chem.* 36 (2020) 132–138.
- [19] O.C. O, E.W. Nthiga, G.K. Muthakia, D. Onyancha, *Int. J. Sci. Res. Chem. Sci.* 8 (2021) 4–9.
- [20] A.Y. Ugya, X. Hua, J. Ma, *Appl. Ecol. Environ. Res.* 17 (2019) 1773–1787.
- [21] M. Harja, G. Buema, D. Bucur, *Sci. Rep.* 12 (2022) 1–18.
- [22] T. Tapalad, A. Neramittagapong, S. Neramittagapong, M. Boonmee, *Chiang Mai J. Sci.* 35 (2008) 63–68.
- [23] S.A. Dhahir, K.A. Al-Saade, I.S. Al-Jobouri, *Anal. Chem. an Indian J.* 15 (2015) 117–124.
- [24] M. Shaban, M.R. Abukhadra, S.S. Ibrahim, M.G. Shahien, *Appl. Water Sci.* 7 (2017) 4743–4756.
- [25] I. Mironyuk, N. Danyliuk, T. Tatarchuk, I. Mykytyn, V. Kotsyubynsky, *Phys. Chem. Solid State* 22 (2021) 697–710.
- [26] T.K. Roy, N.K. Mondal, *Appl. Water Sci.* 7 (2017) 1841–1854.
- [27] W.C. Wanyonyi, J.M. Onyari, P.M. Shiundu, *Energy Procedia* 50 (2014) 862–869.
- [28] E. Zhang, J. Wu, G. Wang, B. Zhang, Y. Xie, *J. Nanosci. Nanotechnol.* 16 (2016) 4727–4732.
- [29] P. Gharbani, S.M. Tabatabaai, A. Mehrizad, *Int. J. Environ. Sci. Technol.* 5 (2008) 495–500.
- [30] P.W. Koh, M.H.M. Hatta, S.T. Ong, L. Yuliati, S.L. Lee, *J. Photochem. Photobiol. A Chem.* 332 (2017) 215–223.
- [31] E.T. Wahyuni, S. Wahyuni, N.D. Lestari, S. Suherman, *React. Kinet. Mech. Catal.* 136 (2023) 1067–1084.
- [32] M. Chowdhury, M.G. Mostafa, T.K. Biswas, A. Mandal, A.K. Saha, *Environ. Process.* 2 (2015) 173–187.